The Astrophysical Journal Letters, 948:L20 (6pp), 2023 May 10 https://doi.org/10.3847/2041-8213/acd0b4

Narrow Loophole for H_2-Dominated Atmospheres on Habitable Rocky Planets around M Dwarfs

Renyu Hu[1,2], Fabrice Gaillard[3], and Edwin S. Kite[4]
[1] Jet Propulsion Laboratory, California Institute of Technology, Pasadena, CA 91109, USA; renyu.hu@jpl.nasa.gov
[2] Division of Geological and Planetary Sciences, California Institute of Technology, Pasadena, CA 91125, USA
[3] Institut des Sciences de la Terre d'Orléans, CNRS/Université d'Orléans/BRGM, 1a rue de la Férollerie, 45071 Orléans cedex 2, France
[4] Department of the Geophysical Sciences, University of Chicago, Chicago, IL 60637, USA
Received 2023 February 26; revised 2023 April 12; accepted 2023 April 26; published 2023 May 11

Abstract

Habitable rocky planets around M dwarfs that have H_2-dominated atmospheres, if they exist, would permit characterizing habitable exoplanets with detailed spectroscopy using JWST, owing to their extended atmospheres and small stars. However, the H_2-dominated atmospheres that are consistent with habitable conditions cannot be too massive, and a moderate-sized H_2-dominated atmosphere will lose mass to irradiation-driven atmospheric escape on rocky planets around M dwarfs. We evaluate volcanic outgassing and serpentinization as two potential ways to supply H_2 and form a steady-state H_2-dominated atmosphere. For rocky planets of 1–7 $M_\oplus$ and early-, mid-, and late M-type dwarfs, the expected volcanic outgassing rates from a reduced mantle fall short of the escape rates by $>\sim 1$ order of magnitude, and a generous upper limit of the serpentinization rate is still less than the escape rate by a factor of a few. Special mechanisms that may sustain the steady-state H_2-dominated atmosphere include direct interaction between liquid water and mantle, heat-pipe volcanism from a reduced mantle, and hydrodynamic escape slowed down by efficient upper-atmospheric cooling. It is thus unlikely to find moderate-size, H_2-dominated atmospheres on rocky planets of M dwarfs that would support habitable environments.

Unified Astronomy Thesaurus concepts: Exoplanet atmospheres (487); Exoplanet surfaces (2118); Extrasolar rocky planets (511); Exoplanet evolution (491); Super Earths (1655); Transmission spectroscopy (2133)

1. Introduction

Rocky planets with H_2-dominated atmospheres would be ideal targets for atmospheric characterization via transmission spectroscopy because of their large atmospheric scale height that causes large expected spectral features (e.g., Miller-Ricci et al. 2008; Seager & Deming 2010; Greene et al. 2016). A moderately irradiated rocky planet with a H_2-dominated atmosphere may have surface pressure and temperature consistent with liquid water (Pierrehumbert & Gaidos 2011; Wordsworth 2012; Ramirez & Kaltenegger 2017; Koll & Cronin 2019). Such potentially habitable worlds sustained by H_2-dominated atmospheres, if they exist around M dwarfs, would unlock the opportunity to study extrasolar habitability with spectroscopy (e.g., Seager et al. 2013), as TESS and ground-based surveys find temperate rocky planets around M dwarfs (e.g., Sebastian et al. 2021; Kunimoto et al. 2022), and JWST provides the sensitivity to analyze any H_2-dominated atmospheres on them with a wide spectral coverage (e.g., Batalha et al. 2018). Here we ask: Are such worlds likely?

To have surface liquid water, the H_2-dominated atmosphere cannot be much larger than $\sim$10 bar because the surface temperature is primarily a function of the size of the atmosphere (this is valid for the stellar irradiation of 200–1400 W m^{-2}; Koll & Cronin 2019). The exact size and irradiation limit depends on the cloud albedo effect (e.g., Popp et al. 2015). This moderate-sized atmosphere is much smaller than the massive H_2-dominated atmospheres proposed to explain the sub-Neptune-sized low-density planet population, which are typically 1% planet mass or $>10^4$ bar (e.g., Rogers et al. 2023). A 10 bar H_2 atmosphere would only add $<\sim 0.1\,R_\oplus$ to the planetary radius, which can be accommodated by typical uncertainties in planetary mass, radius, and Fe content (Luque & Pallé 2022). Also, the temperate rocky planets will have a solid surface, as opposed to the sub-Neptunes that may have a permanent magma ocean (Kite & Barnett 2020). Because the permeability of the crust decreases dramatically with increasing depth (Manning & Ingebritsen 1999), any post-formation source of H_2 must come from shallow fresh crust via either volcanic outgassing or crustal alteration processes such as serpentinization.

Meanwhile, temperate planets around M dwarfs receive intense high-energy irradiation from host stars because of their close-in orbits, and this intense irradiation can drive hydrodynamic escape from a H_2-dominated atmosphere (e.g., Salz et al. 2016; Kubyshkina et al. 2018a, 2018b). The high-energy irradiation will be measured by a bevy of new spacecraft (Ardila et al. 2022; France et al. 2023). We are thus motivated to determine the lifetime of a moderate-sized H_2 atmosphere—permitting surface liquid water—on a large rocky planet orbiting an M dwarf against the hydrodynamic escape and evaluate the geologic processes that could resupply the H_2 atmosphere.

2. Atmospheric Escape

The hydrodynamic escape rate, f_{es} (kg s^{-1}), can be approximated by the energy-limited escape rate formula,

$$f_{es} = \frac{\eta_{es}(F_X + F_{EUV})\pi R_p^3 a^2}{KGM_p}, \quad (1)$$

Table 1
Lifetimes and Required Hydrogen Outgassing for Thin H2 Atmospheres of M Dwarf Rocky Planets

Star	Type	F (erg s^{-1} cm^{-2})		f_{es} (10^4 kg s^{-1})			Life of 10 bar atmosphere (Gyr)			Required x_H (wt%)		
		X-Ray	EUV	1 $M_\oplus$	3 $M_\oplus$	7 $M_\oplus$	1 $M_\oplus$	3 $M_\oplus$	7 $M_\oplus$	1 $M_\oplus$	3 $M_\oplus$	7 $M_\oplus$
GJ 832	M1.5	2.17	149	3.1	2.3	2.2	0.05	0.07	0.09	9.2	1.7	0.35
GJ 436	M3.5	8.71	229	4.9	3.6	3.4	0.03	0.04	0.06	14	2.7	0.54
TRAPPIST-1	M8	171	1097*	26	19	18	0.006	0.008	0.01	77	14	2.9

Note. Escape rates and lifetimes of a 10 bar H_2 atmosphere, and the required hydrogen content in magma for degassing to sustain this atmosphere, on a hypothetical rocky planet of an M dwarf. The distance between the planet and the star results in a bolometric stellar flux the same as Earth's insolation (i.e., the 1 au equivalent distance). The X-ray fluxes (5–100 Å) are measured by XMM-Newton (Ehrenreich et al. 2015; Loyd et al. 2016; Wheatley et al. 2017) and the EUV fluxes (100–1240 Å) are based on PHOENIX synthetic spectra guided by FUV and NUV observations (Peacock et al. 2019b, 2019a). *Bourrier et al. (2017) reported a much lower EUV flux (126 erg s^{-1} cm^{-2} at TRAPPIST-1 e) based on Lyα measurements, but using this lower value does not change the conclusion of this paper.

where F_X and F_{EUV} are the stellar fluxes in X-ray (5–100 Å) and extreme ultraviolet (EUV; 100–1240 Å), $a \geqslant 1$ is the ratio between the X-ray/EUV absorbing radius and the (optical) planetary radius, $K \leqslant 1$ is a factor that accounts for the Roche lobe effect (Erkaev et al. 2007), and η_{es} is the escape efficiency. Recent hydrodynamic escape models find the escape efficiency to be in a range of 0.1–0.25 for solar-abundance atmospheres (Salz et al. 2016), and Equation (1) is a good approximation of the full hydrodynamic calculations in the Jeans escape parameter regime for temperate rocky planets (Jeans escape parameter = 25–60; Kubyshkina et al. 2018a, 2018b). For a conservative estimate of the escape rate, we adopt $\eta_{es} = 0.1$, $a = 1$, and $K = 1$.

As shown in Table 1, we pick GJ 832, GJ 436, and TRAPPIST-1 as the representative stars for early-, mid-, and late-type M dwarfs. Their emission spectra in X-ray, Lyα, far-ultraviolet (FUV), and near-ultraviolet (NUV) bands have been measured, and their emission spectra and fluxes in the EUV band can be inferred from these measurements (Peacock et al. 2019b, 2019a). We find that the lifetime of a 10 bar H_2 atmosphere on a rocky planet that receives Earth-like insolation from these stars would be uniformly <0.1 Ga. Thus, a source of H_2 would be needed to maintain such an atmosphere.

3. Volcanic Outgassing

We first consider volcanic outgassing as the source of H_2 (e.g., Liggins et al. 2020). The volcanic outgassing rate, f_{og} (kg s^{-1}), can be modeled by the following equation,

$$f_{og} = \eta_{og} V x_H, \quad (2)$$

where V is the rate of magma generation, x_H is the hydrogen content (wt%) of magma that degasses, and η_{og} is the outgassing efficiency. We do not expect the outgassing efficiency to be close to unity because, even though extrusive volcanism (magma that reaches and degases at the planetary surface) can probably degas effectively (but often not completely), intrusive volcanism (magma that does not reach the surface) probably degases poorly, especially for H_2 (to be detailed later in this section). For Earth, the extrusive:intrusive ratio is typically 3:1 to 10:1 (White et al. 2006), and so as a fiducial value, we assume $\eta_{og} = 0.1$.

The rate of volcanism can be estimated for a rocky planet by modeling its thermal evolution history. We adopt the geodynamics model of Kite et al. (2009) for the rate of volcanism, which used a melting model from pMELTS (Ghiorso et al. 2002) for the plate tectonic mode and Katz et al. (2003) for the stagnant-lid mode (Table 2). Focusing first on the planets around field M dwarfs, we take the 4 Gyr age values for the rate of volcanism. The values for the plate tectonic and stagnant-lid modes are similar. Detailed models of mantle convection in the stagnant-lid regime predict that volcanism would cease much sooner than what Table 2 indicates (Noack et al. 2017; Dorn et al. 2018), but this model uncertainty does not impact the conclusion of this paper. For volcanic outgassing to sustain the atmosphere, it is required that $f_{es} = f_{og}$. With f_{es} and V, we derive the required x_H and list the values in Table 1.

Arc volcanoes on Earth, which are formed by flux melting caused by release of water from subduction of plates rich in hydrated materials, have magmas that contain 1–7 wt% water (e.g., Rasmussen et al. 2022). The water content in the mid-ocean ridge basalt (MORB) and the ocean island basalt (OIB) is lower by 1–2 orders of magnitude (Dixon et al. 2002). Complete outgassing of 1–7 wt% water in the form of H_2 would provide an x_H of 0.1–0.8 wt%. We consider this to be a very generous upper limit; comparing it with Table 1 shows that it is very unlikely for volcanic outgassing to sustain the H_2 atmosphere.

The hydrogen content of the magma for degassing depends on the oxygen fugacity of the magma and the pressure at which degassing takes place. We use the magma degassing and speciation model of Gaillard & Scaillet (2014) to calculate x_H for the typical volatile content of terrestrial magmas and a wide range of oxygen fugacities (Figure 1). The H_2 content is higher for a more reducing magma and when degassing at a lower pressure. In addition to counting the H_2 degassing, one may also include the potential for atmospheric photochemistry to postprocess CO to form H_2, via $CO + H_2O \rightarrow CO_2 + H_2$. The complete postprocessing means that degassing 1 mole CO would be equivalent to degassing 1 mole H_2, and this situation is shown as dashed lines in Figure 1. However, x_H predicted by the geochemical model, even when including the CO conversion, is at least 1 order of magnitude lower than the minimum required x_H for a $7M_\oplus$ planet around an early M dwarf (Table 1). This again indicates that volcanic outgassing is unlikely to sustain a H_2 atmosphere.

4. Serpentinization

We turn to serpentinization as an alternative source of H_2. Serpentinization is water–rock reactions between warm water

Table 2
Rate of Volcanism Expected for Rocky Planets

Mode	Plate Tectonics			Stagnant Lid		
Age (Gyr)	2	4	6	2	4	6
1 $M_\oplus$, 1 $R_\oplus$	8	1.5	0.5	7	1.5	0
3 $M_\oplus$, 1.3 $R_\oplus$	⋯	2	0.7	⋯	2.5	0
7 $M_\oplus$, 1.7 $R_\oplus$	⋯	4	1	⋯	3.5	0.7

Note. Rate of volcanism (the mass of magma production divided by the mass of planet, in unit of current Earth's value 3.7516×10^{-19} s^{-1}), based on the parameterized model of Kite et al. (2009). Dashes correspond to the heat-pipe tectonic regime.

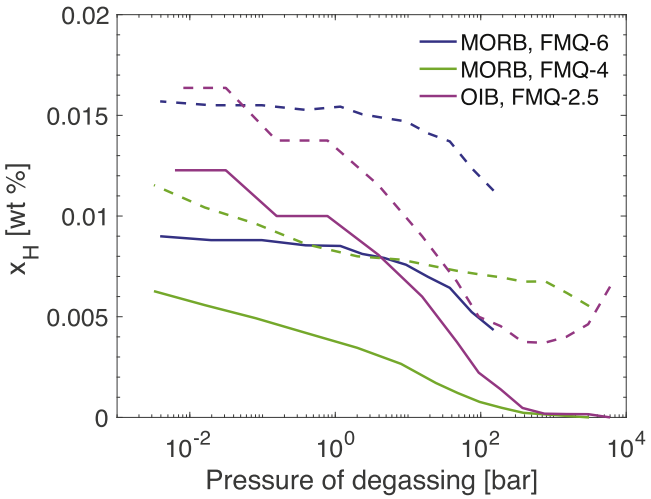

Figure 1. Degassing of H_2 from magma calculated by the magma degassing and speciation model of Gaillard & Scaillet (2014). We consider mid-ocean ridge basalt (MORB) with bulk H_2O content of 0.19 wt% and bulk CO_2 content of 0.16 wt%, degassing at the oxygen fugacities of FMQ-6 (corresponding to an undifferentiated planet) and FMQ-4 (corresponding to modern Mars), as well as ocean island basalt (OIB) with bulk H_2O content of 1 wt% and bulk CO_2 content of 0.3 wt%, degassing at the oxygen fugacities of FMQ-2.5. The solid lines count the degassing of H_2, and the dashed lines count the degassing of both H_2 and CO (with CO expressed in terms of its indirect effect on atmospheric H_2, see Section 3).

and mafic and ultramafic rocks (usually olivine-rich) in the fresh crust. This process probably occurs on all rocky planets with liquid water, and it may have produced H_2-rich water on early Earth (Sleep et al. 2004) and H_2 and CH_4 on early Mars and on modern Enceladus (Oze & Sharma 2005; Chassefière & Leblanc 2011; Batalha et al. 2015; Zandanel et al. 2021).

For an upper bound of the H_2 production rate from serpentinization, we assume that 1 mole H_2 is produced for every 3 moles Fe^{2+} oxidized, as the process can be written as $H_2O + 3FeO \rightarrow H_2 + Fe_3O_4$. We also assume that the fresh crust is entirely composed of olivine, $(Mg_{0.9}Fe_{0.1})_2SiO_4$, and all Fe^{2+} is used by serpentinization to produce H_2. The olivine has a molar mass of 146.9 g, and it contains 0.2 moles Fe^{2+}, corresponding to 0.067 moles H_2, or a mass of 0.13 g. The corresponding x_H is thus $0.13/146.9 = 0.09$ wt%. In reality, the fresh crust may not be entirely composed of olivine, and the rate of serpentinization is limited by the rate of dissolution of olivine in water (Oze & Sharma 2007), which is a function of temperature, pH, water/rock ratio, and the Fe/Mg composition of olivine (Wogelius & Walther 1992; Allen & Seyfried 2003), as well as by the extent of fracturing of the crust (Vance et al. 2007). We thus expect the actual x_H provided by serpentinization to be much smaller than 0.09 wt%. However, even this generous upper bound falls short of the required x_H by at least a factor of 4 (Table 1). It is thus also unlikely that serpentinization would sustain a moderate-sized H_2 atmosphere on rocky planets around M dwarfs.

5. Age and Distance Dependency

So far we have assumed 4 Gyr for the planet age, which broadly corresponds to the field M dwarfs. Now we consider the age dependency of the sources and sinks of H_2 and see if a steady-state H_2 atmosphere would be possible on younger planets. Richey-Yowell et al. (2019) recently presented the NUV, FUV, and X-ray fluxes of M dwarfs in their habitable zones as a function of age, and meanwhile, the EUV fluxes follow a similar age dependency as their FUV fluxes (Peacock et al. 2020). We adopt an age dependency of $t^{-0.9}$ for the X-ray fluxes and $t^{-1.3}$ for the EUV fluxes. Meanwhile, the rate of volcanism can be much higher for young planets, when the heat flux from the planetary interior is higher. We explore an age dependency that varies between t^{-1} (based on the model for Earth in Schubert et al. 2001) and t^{-2} (based on the model for large rocky planets of Kite et al. 2009). We consider an age as young as 1 Gyr. Before that, the planet could have a residual primordial H_2 atmosphere (Kite & Barnett 2020), and the stellar high-energy output may have different age dependencies (Richey-Yowell et al. 2019). As shown in Figure 2, it remains unlikely for volcanic outgassing or serpentinization to compensate for the intense atmospheric escape of H_2 experienced by rocky planets of M dwarfs from 1 to 5 Gyr.

How about a planet that is located further away from the star than the 1 au equivalent distance? Moving the planets 2.6 times further away (or receiving 7 times less irradiation, or ∼200 W m^{-2}) would still produce a potentially habitable climate (Koll & Cronin 2019), and this would reduce the escape rate by a factor of 7. In this case, the escape rate is comparable to the upper limit of serpentinization (Figure 2). However, the upper limit assumes complete oxidization of Fe^{2+} in the fresh crust and is thus unlikely. The utility of these distant habitable worlds for observations is probably limited, as they are less likely to transit and harder to find than the closer-in planets.

6. Potential Alternative Mechanisms

The estimates above show that it is unlikely to sustain moderate-sized H_2-dominated atmospheres on rocky planets around M dwarfs through volcanic outgassing or serpentinization. Here we explore alternative mechanisms that could result in large source fluxes of H_2.

First, the rate of hydrogen generation during serpentinization is controlled by the Fe content of olivine (Klein et al. 2013). In Section 4, we have assumed an Fe:Mg ratio of 1:9, corresponding to the terrestrial value. On Mars, however, the Fe:Mg ratio of crustal olivine can be ∼1:1 (Koeppen & Hamilton 2008; Morrison et al. 2018). Such Fe-rich olivine could result in higher fluxes of H_2 from serpentinization than our estimates by a factor of ∼5, making it more likely for serpentinization to meet the H_2 escape flux.

Second, on a planet with plate tectonics but amagmatic spreading, water–rock interaction near the ridge axis could produce H_2. Our discussion of serpentinization so far assumes that water interacts with the products of volcanism/partial melting. However, water could interact directly with the mantle

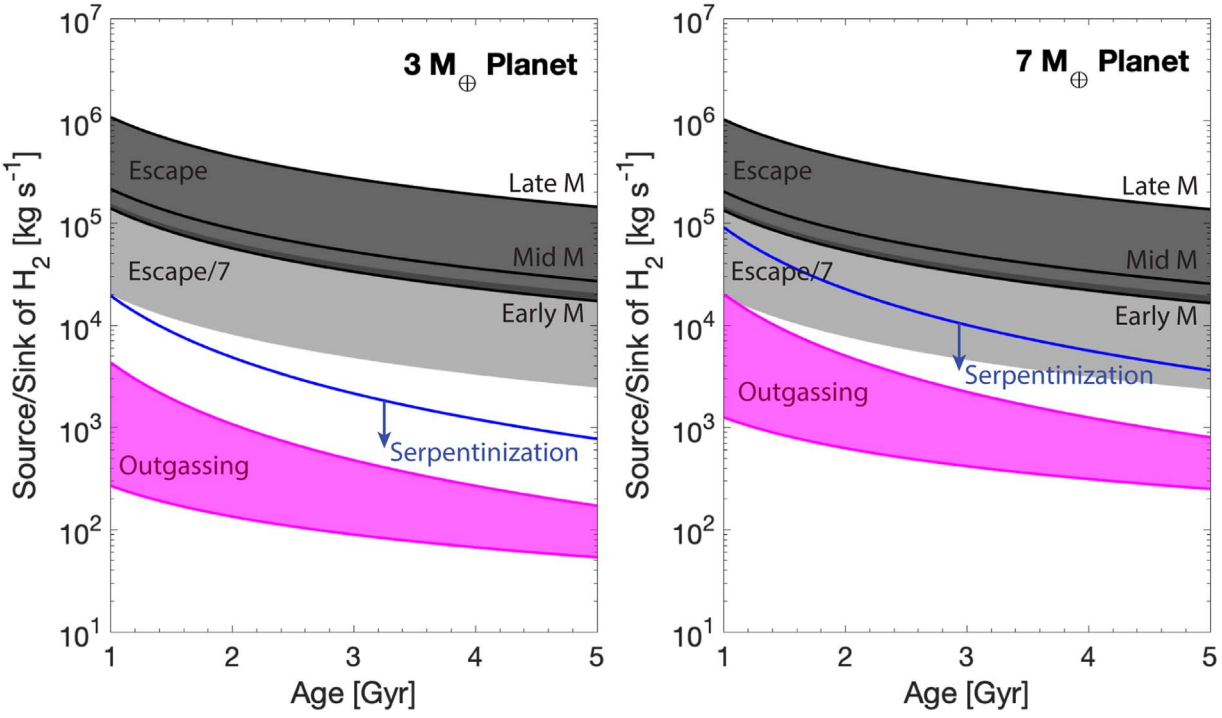

Figure 2. Comparison between sources and sinks of H_2 on rocky planets around M dwarfs. The gray areas show the range of escape rates depending on the type of the host star. The dark gray area is for a planet that locates at the 1 au equivalent distance, while the light gray area is for a planet that locates 2.6 times farther away (i.e., receiving 7 times less irradiation). The outgassing rates encapsulate the plausible range from a highly reduced mantle (informed by Figure 1), with the lower bound corresponding to $x_H = 0.005$ wt% and t^{-1} scaling, and the higher bound corresponding to $x_H = 0.02$ wt% and t^{-2} scaling. The rate of serpentinization is a very generous upper limit (Section 4).

if it is exposed by amagmatic spreading. This mechanism occurs on Earth today at Gakkel Ridge and Southwest Indian Ridge and has the potential to generate more H_2 because the Fe content of mantle rock is greater than that of the crustal basalt. This mechanism would decouple serpentinization from volcanism and allow serpentinization to continue even after volcanism has shut down. The upper limit of H_2 production from this mechanism is then given by assuming (unrealistically) a 100% fayalite (Fe_2SiO_4), which would give an equivalent x_H of 0.6 wt%. Suppose fractures, and therefore hot-water alteration, penetrate as far down into the subsurface on this amagmatic planet as the base of the oceanic crust on our planet, which is probably unrealistic because fractures should self-seal at shallower depths (Vance et al. 2007). Then the present-day terrestrial production of 20 $km^3\,yr^{-1}$ of MORB, with full serpentinization, would correspond to 1×10^4 kg s^{-1} of H_2 output. This is on the same order of magnitude as the lower end of the escape rate (Table 1) and could be higher for younger or larger rocky planets.

Third, Earth's heat flux of ~0.1 W m^{-2} is ~10% in the form of advective cooling (magma moves upward and cools) and ~90% conductive cooling. This implies that the rates of volcanism could be 10 × higher without excessively cooling Earth's mantle. Indeed, it has been hypothesized that heat-pipe tectonics occurred early in Earth's history (e.g., Moore & Webb 2013). Small variations in exoplanet mantle composition or exoplanet mantle volatile content, among other factors, could make melting easier at a given mantle temperature (Spaargaren et al. 2020), perhaps enabling heat-pipe mode of planetary cooling even for planets that are as old as the Earth. If heat-pipe volcanism occurs, then the amount of outgassing and serpentinization could be ~10 × greater than for an Earth-scaled plate-tectonics model because ~10 × more eruptions would occur.

Fourth, N-, O-, and C-bearing molecules mixed in the H_2-dominated atmosphere may substantially reduce the escape rate. The escape rate and efficiency calculations have been based on solar-abundance atmospheres (Kubyshkina et al. 2018a, 2018b). However, H_2-dominated atmospheres sustained by volcanism should also have H_2O, CO/CH_4, and N_2/NH_3 at the levels that exceed the solar abundance (Liggins et al. 2022). Recently, Nakayama et al. (2022) show that with an N_2–O_2 atmosphere, cooling from atomic line emissions (of N, N^+, O, O^+) and radiative recombination can prevent rapid hydrodynamic escapes for XUV irradiation fluxes that are up to 1000 × the modern Earth value. It is thus conceivable that an H_2-dominated atmosphere richer in N, O, and C would be more stable. The challenge is that the N-, O-, and C-bearing molecules are separated from H_2 by diffusion (typically at ~1 Pa) and can be largely depleted in the upper atmosphere. It is thus unclear whether 10% non-H_2 species (which would still allow for a low molecular weight atmosphere for transmission spectroscopy) would slow down the hydrodynamic escape sufficiently to achieve long-term stability.

Lastly, there could be transient episodes of high volcanism and serpentinization that support H_2-dominated atmospheres. A leading hypothesis for why early Mars sometimes had lakes is that a lot of H_2 was emitted transiently from the subsurface by volcanism or serpentinization (Wordsworth et al. 2021). The amount of H_2 needed to warm up Mars by H_2–CO_2 collision-induced absorption is now well understood (Turbet et al. 2020), and the H_2 flux needed is approximately 10^4 kg s^{-1}. A large rocky planet could have 10 × the surface area of Mars and thus plausibly 10 × the amount of serpentinization. This process-

agnostic (but model-dependent) scaling hints at short-term source fluxes sufficient for H_2-dominated atmospheres on a $7M_\oplus$ planet (Figure 2).

7. Summary

From the analyses presented above, we conclude that rocky planets around M dwarfs rarely have potentially habitable conditions accompanied by H_2-dominated atmospheres. This is because forming a potentially habitable environment will require a moderate-sized (∼10 bar) atmosphere, but such an atmosphere is removed quickly by stellar X-ray and EUV irradiation and could only exist on the planet as a steady-state atmosphere with replenishment. However, neither volcanic outgassing nor serpentinization provides the required H_2 source that would maintain such a steady-state atmosphere. Small planets around M dwarfs could have massive H_2 atmospheres, but to have a stable and moderate-sized H_2 atmosphere consistent with habitability would require special circumstances such as direct interaction between liquid water and mantle (e.g., near a ridge axis undergoing amagmatic spreading), heat-pipe volcanism from a highly reduced mantle, or hydrodynamic escape quenched by efficient atomic line cooling. These special mechanisms to sustain the moderate-sized H_2 atmosphere are generally more effective on large rocky planets (e.g., $\sim 7M_\oplus$ planets exemplified by LHS 1140b) than on Earth-sized planets.

The finding here is consistent with the nondetection to date of clear H_2-dominated atmospheres on rocky planets of M dwarfs via transmission spectroscopy (e.g., De Wit et al. 2018; Lustig-Yaeger et al. 2023) although these results could also be interpreted as widely occurring photochemical haze that mutes transmission spectral features of H_2-dominated atmospheres. Swain et al. (2021) suggested a H_2-dominated atmosphere on the rocky planet GJ 1132 b based on Hubble Space Telescope (HST) data, but independent data analyses could not confirm their result (Mugnai et al. 2021; Libby-Roberts et al. 2022). The ongoing HST and JWST transmission spectroscopy of small exoplanets of M dwarfs will further test our findings and, potentially, discover exceptional cases. Meanwhile, N_2–CO_2 or other high mean molecular weight atmospheres should probably be considered as the default assumption when planning for future spectroscopic observations of rocky planets around M dwarfs. This would require planning more repeated visits of preferred targets for transmission spectroscopy (e.g., Batalha et al. 2018) or turning to thermal emission spectroscopy and phase-curve mapping (e.g., Angelo & Hu 2017; Koll et al. 2019; Kreidberg et al. 2019; Mansfield et al. 2019; Whittaker et al. 2022).

We thank Evgenya Shkolnik and Tyler Richey-Yowell for helpful discussion of stellar evolution. This work was supported in part by the NASA Exoplanets Research Program grant #80NM0018F0612. E.S.K. acknowledges support from a Scialog grant, Heising-Simons Foundation 2021–3119. Part of this research was carried out at the Jet Propulsion Laboratory, California Institute of Technology, under a contract with the National Aeronautics and Space Administration.

ORCID iDs

Renyu Hu https://orcid.org/0000-0003-2215-8485
Edwin S. Kite https://orcid.org/0000-0002-1426-1186

References

Allen, D. E., & Seyfried, W., Jr. 2003, GeCoA, 67, 1531
Angelo, I., & Hu, R. 2017, AJ, 154, 232
Ardila, D. R., Shkolnik, E., Scowen, P., et al. 2022, arXiv:2211.05897
Batalha, N., Domagal-Goldman, S. D., Ramirez, R., & Kasting, J. F. 2015, Icar, 258, 337
Batalha, N. E., Lewis, N. K., Line, M. R., Valenti, J., & Stevenson, K. 2018, ApJL, 856, L34
Bourrier, V., Ehrenreich, D., Wheatley, P., et al. 2017, A&A, 599, L3
Chassefière, E., & Leblanc, F. 2011, E&PSL, 310, 262
De Wit, J., Wakeford, H. R., Lewis, N. K., et al. 2018, NatAs, 2, 214
Dixon, J. E., Leist, L., Langmuir, C., & Schilling, J.-G. 2002, Natur, 420, 385
Dorn, C., Noack, L., & Rozel, A. 2018, A&A, 614, A18
Ehrenreich, D., Bourrier, V., Wheatley, P. J., et al. 2015, Natur, 522, 459
Erkaev, N., Kulikov, Y. N., Lammer, H., et al. 2007, A&A, 472, 329
France, K., Fleming, B., Egan, A., et al. 2023, AJ, 165, 63
Gaillard, F., & Scaillet, B. 2014, E&PSL, 403, 307
Ghiorso, M. S., Hirschmann, M. M., Reiners, P. W., & Kress, V. C., III 2002, GGG, 3, 1030
Greene, T. P., Line, M. R., Montero, C., et al. 2016, ApJ, 817, 17
Katz, R. F., Spiegelman, M., & Langmuir, C. H. 2003, GGG, 4, 8705
Kite, E. S., & Barnett, M. N. 2020, PNAS, 117, 18264
Kite, E. S., Manga, M., & Gaidos, E. 2009, ApJ, 700, 1732
Klein, F., Bach, W., & McCollom, T. M. 2013, Litho, 178, 55
Koeppen, W. C., & Hamilton, V. E. 2008, JGRE, 113, E05001
Koll, D. D., & Cronin, T. W. 2019, ApJ, 881, 120
Koll, D. D., Malik, M., Mansfield, M., et al. 2019, ApJ, 886, 140
Kreidberg, L., Koll, D. D., Morley, C., et al. 2019, Natur, 573, 87
Kubyshkina, D., Fossati, L., Erkaev, N. V., et al. 2018a, A&A, 619, A151
Kubyshkina, D., Fossati, L., Erkaev, N. V., et al. 2018b, ApJL, 866, L18
Kunimoto, M., Winn, J., Ricker, G. R., & Vanderspek, R. K. 2022, AJ, 163, 290
Libby-Roberts, J. E., Berta-Thompson, Z. K., Diamond-Lowe, H., et al. 2022, AJ, 164, 59
Liggins, P., Jordan, S., Rimmer, P. B., & Shorttle, O. 2022, JGRE, 127, e07123
Liggins, P., Shorttle, O., & Rimmer, P. B. 2020, E&PSL, 550, 116546
Loyd, R. P., France, K., Youngblood, A., et al. 2016, ApJ, 824, 102
Luque, R., & Pallé, E. 2022, Sci, 377, 1211
Lustig-Yaeger, J., Fu, G., May, E., et al. 2023, arXiv:2301.04191
Manning, C., & Ingebritsen, S. 1999, RvGeo, 37, 127
Mansfield, M., Kite, E. S., Hu, R., et al. 2019, ApJ, 886, 141
Miller-Ricci, E., Seager, S., & Sasselov, D. 2008, ApJ, 690, 1056
Moore, W. B., & Webb, A. A. G. 2013, Natur, 501, 501
Morrison, S. M., Downs, R. T., Blake, D. F., et al. 2018, AmMin, 103, 857
Mugnai, L. V., Modirrousta-Galian, D., Edwards, B., et al. 2021, AJ, 161, 284
Nakayama, A., Ikoma, M., & Terada, N. 2022, ApJ, 937, 72
Noack, L., Rivoldini, A., & Van Hoolst, T. 2017, PEPI, 269, 40
Oze, C., & Sharma, M. 2005, GeoRL, 32, L10203
Oze, C., & Sharma, M. 2007, Icar, 186, 557
Peacock, S., Barman, T., Shkolnik, E. L., et al. 2019a, ApJ, 886, 77
Peacock, S., Barman, T., Shkolnik, E. L., et al. 2020, ApJ, 895, 5
Peacock, S., Barman, T., Shkolnik, E. L., Hauschildt, P. H., & Baron, E. 2019b, ApJ, 871, 235
Pierrehumbert, R., & Gaidos, E. 2011, ApJL, 734, L13
Popp, M., Schmidt, H., & Marotzke, J. 2015, JAtS, 72, 452
Ramirez, R. M., & Kaltenegger, L. 2017, ApJL, 837, L4
Rasmussen, D. J., Plank, T. A., Roman, D. C., & Zimmer, M. M. 2022, Sci, 375, 1169
Richey-Yowell, T., Shkolnik, E. L., Schneider, A. C., et al. 2019, ApJ, 872, 17
Rogers, J. G., Schlichting, H. E., & Owen, J. E. 2023, ApJL, 947, L19
Salz, M., Schneider, P., Czesla, S., & Schmitt, J. 2016, A&A, 585, L2
Schubert, G., Turcotte, D. L., & Olson, P. 2001, Mantle Convection in the Earth and Planets (Cambridge: Cambridge Univ. Press)
Seager, S., Bains, W., & Hu, R. 2013, ApJ, 777, 95
Seager, S., & Deming, D. 2010, ARA&A, 48, 631
Sebastian, D., Gillon, M., Ducrot, E., et al. 2021, A&A, 645, A100
Sleep, N., Meibom, A., Fridriksson, T., Coleman, R., & Bird, D. 2004, PNAS, 101, 12818
Spaargaren, R. J., Ballmer, M. D., Bower, D. J., Dorn, C., & Tackley, P. J. 2020, A&A, 643, A44
Swain, M. R., Estrela, R., Roudier, G. M., et al. 2021, AJ, 161, 213
Turbet, M., Boulet, C., & Karman, T. 2020, Icar, 346, 113762
Vance, S., Harnmeijer, J., Kimura, J., et al. 2007, AsBio, 7, 987

Wheatley, P. J., Louden, T., Bourrier, V., Ehrenreich, D., & Gillon, M. 2017, MNRAS: Letters, 465, L74
White, S. M., Crisp, J. A., & Spera, F. J. 2006, GGG, 7, Q03010
Whittaker, E. A., Malik, M., Ih, J., et al. 2022, AJ, 164, 258
Wogelius, R. A., & Walther, J. V. 1992, ChGeo, 97, 101
Wordsworth, R. 2012, Icar, 219, 267
Wordsworth, R., Knoll, A. H., Hurowitz, J., et al. 2021, NatGe, 14, 127
Zandanel, A., Truche, L., Hellmann, R., et al. 2021, Icar, 364, 114461